DOI: 10.1002/anie.200904300

Polymerization

Metalloorganic Polymerization Catalysis as a Tool To Probe Crystallization Properties of Polymers: The Case of Isotactic Poly(1-butene)**

Claudio De Rosa, Finizia Auriemma, and Luigi Resconi*

The discovery and development of metalloorganic catalysis have allowed increasing control over the microstructure of polymer chains with a relevant impact on the final material properties.[1,2] A major evolution has occurred in the production of poly(propylene), whose properties can be tailored in the polymerization stage by using metalloorganic catalysts with appropriate structures. However, this process requires profound insight into the relationships between catalyst structure, chain microstructure, crystallization properties, and properties of the final product. The usefulness of single-center metallocene catalysts in achieving this objective has been recently demonstrated in the case of isotactic polypropylene (iPP).[3] Metallocene catalysts, indeed, afford the controlled random incorporation of a single type of microstructural defects (*stereo* and *regio* defects as well as constitutional defects),[2,4] allowing study of the influence of defects on the crystallization and physical properties of iPP.[3] Although the huge commercial success of iPP is due to the continuous development of traditional Ziegler–Natta catalysts, the vast majority of products being fabricated with the highly isotactic polymer, a range of polypropylenes with properties not accessible with Ziegler–Natta catalysts, have been produced with metallocene catalysts.

In contrast with iPP, all the extensive investigations on the development of different generations of Ziegler–Natta catalysts have produced only limited commercial success of isotactic polybutene (iPB), its attractive physical properties notwithstanding. In fact, iPB exhibits advantages over other polyolefins, such as polyethylene and polypropylene, in superior toughness, tear strength, flexibility, creep, and impact resistance and finds many applications in, for example, pressurized tanks, tubes, and hot water pipes. However, these useful properties belong to the stable, denser trigonal form I (Figure 1 A),[5] which forms upon spontaneous solid-phase transformation at room temperature of the metastable, kinetically favored tetragonal form II (Figure 1 B),[6,7] formed by crystallization from the melt. This transformation requires several days to go to completion[8] and produces undesirable effects, such as shrinkage of the molded objects as a result of densification.[8] These drawbacks have considerably limited the application of iPB and prevented its broader commercial diffusion, and a great deal of research has thus been oriented towards finding solutions to accelerate the transition.

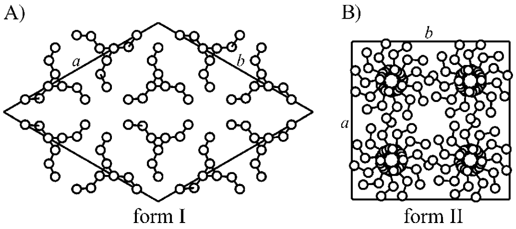

Figure 1. Crystal structures of A) the trigonal form I, with 3_1 helical chains, and B) tetragonal form II, with 11_3 helical chains, of iPB.

Herein, we show that the use of metallocene catalysts applied to 1-butene polymerization produces iPB samples that can be used as model systems for understanding the crystallization behavior of this polymer, and in particular for probing the thermodynamic and kinetics factors that govern the crystallization of polymers and spontaneous phase transformations. This research is the key for finding solutions to the complex polymorphic transition of iPB that still stands in the way of the commercial development of iPB.

Samples of iPB of different stereoregularity have been prepared with the C_1-symmetric metallocene catalysts **1**–**8** in liquid 1-butene in the polymerization temperature range 50–90 °C. The appropriate choice of metallocene catalyst can provide iPB with molecular masses covering the whole range of practical interest for industrially significant polymerization conditions.[9] Moreover, the structure of the catalysts can be modified to tune the polymer stereoregularity, and samples containing one type of stereoirregularity, namely, *rr* triad defects,[9] have been produced with *rr* concentrations between 0.3 and 5 % and melting temperatures in the range 125–70 °C. A list of the samples with characterization details of the polymer is reported in Table 1.

The X-ray powder diffraction profiles of the iPB samples, crystallized from the melt by cooling the melt to room temperature at 2.5 °C min^{-1}, are reported in Figure 2 A. The diffraction profiles of the same melt-crystallized samples aged at room temperature for 1 month are reported in Figure 2 B.

---

[*] Prof. C. De Rosa, Prof. F. Auriemma
Dipartimento di Chimica “Paolo Corradini”
Università di Napoli “Federico II”
Complesso Monte Sant’ Angelo, via Cintia, 80126 Napoli (Italy)
Fax: (+39) 081-674-090/345
E-mail: claudio.derosa@unina.it

Dr. L. Resconi[+]
Basell Polyolefins, Centro Ricerche G. Natta, Ferrara (Italy)

[+] Present address: Borealis Polyolefine GmbH, Linz (Austria)

[**] Financial support from Basell Polyolefins (Italy) and MIUR (PRIN 2007) are gratefully acknowledged.

Supporting information for this article is available on the WWW under http://dx.doi.org/10.1002/anie.200904300.

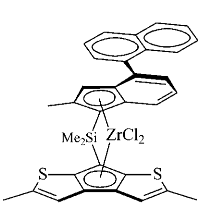

1

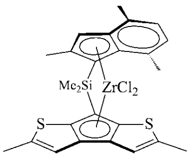

2

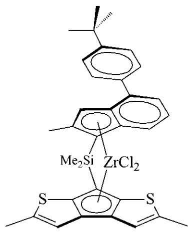

3

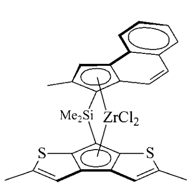

4

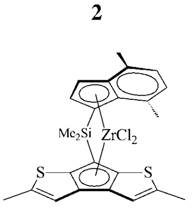

5

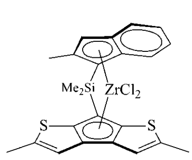

6

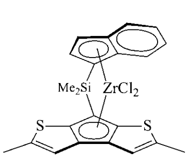

7

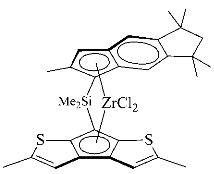

8

Table 1: Characterization data for the iPB samples prepared with catalysts **1**–**8**.

Sample	Cat.	M_v[a]	M_w[b]	M_w/M_n[c]	4m [%][d]	rr [%][e]	T_m(I) [°C][f]	x_c [%][g]
iPB**1**	**1**	204 000	236 000	2.0	98.0	0.4	125	66
iPB**2**	**2**	229 000	297 000	2.1	96.2	0.8	120	63
iPB**3**	**3**	243 000	315 000	2.0	94.2	1.2	115	64
iPB**4**	**4**	321 000	414 000	2.0	92.2	1.4	113	61
iPB**5**	**5**	189 000	228 000	2.0	87.7	2.5	103	52
iPB**6**	**6**	134 000	176 000	2.2	86.5	2.8	99	50
iPB**7**	**7**	132 000	173 000	2.1	77.7	4.7	92	44
iPB**8**	**8**	216 000	280 000	2.1	76.1	5.0	71	44

[a] Viscosity average molecular mass. [b] Mass average molecular mass. [c] Polydispersity. [d] Concentration of the isotactic *mmmm* pentad. [e] Concentration of *rr* triad. [f] Melting temperature of sample in form I crystallized from the melt and aged at room temperature for long time. [g] X-ray crystallinity of melt-crystallized samples.

It is apparent that all the more stereoregular samples with concentrations of *rr* stereodefects lower than 1.4 mol% crystallize from the melt into form II,[6,7] as indicated by the presence of the $(200)_{II}$, $(220)_{II}$, and $(213)_{II}+(311)_{II}$ reflections at $2\theta=11.9$, 16.9, and 18.3°, respectively, in the diffraction profiles a–d of Figure 2A. The crystallization of the metastable form II from the melt is the common behavior of iPB observed in samples of iPB prepared with Ziegler–Natta catalysts and extensively described in the literature.[8]

Less stereoregular samples crystallize from the melt instead in the stable form I,[5] as indicated by the presence of $(110)_I$, $(300)_I$, and $(220)_I+(211)_I$ reflections of form I at $2\theta=9.9$, 17.3, and 20.5°, respectively, in the diffraction profiles e–h of Figure 2A. The presence of *rr* stereodefects in concentrations higher than 2 mol% induces the crystallization from the melt of form I instead of the metastable form II.

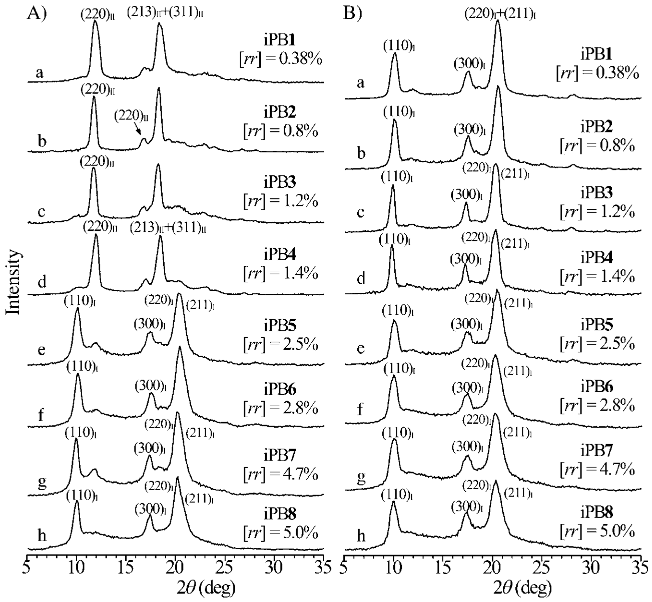

Figure 2. X-ray powder diffraction profiles of samples of iPB of different stereoregularity crystallized by cooling the melt to room temperature (or lower temperature) at a cooling rate of 2.5 °C min^{-1} recorded soon after the cooling (A) and after aging at room temperature for at least 1 month (B). The $(110)_I$, $(300)_I$, and $(220)_I+(211)_I$ reflections of form I at $2\theta=9.9$, 17.3, and 20.5°, respectively, and the $(200)_{II}$, $(220)_{II}$, and $(213)_{II}+(311)_{II}$ reflections of form II at $2\theta=11.9$, 16.9, and 18.3°, respectively, are indicated. All spectra are vertically displaced.

To demonstrate that crystals of form I are obtained in stereodefective iPB samples directly from the melt and not from rapid transformation of form II, time-resolved X-ray diffraction experiments during the melt crystallization were performed. Since the reflections diagnostic of crystals of form I and form II are in the diffraction angle range $2\theta=9$–13° ($(110)_I$ reflection of form I at $2\theta=9.9$° and $(200)_{II}$ reflection of form II at $2\theta=11.9$°), the diffraction profiles were recorded during the isothermal crystallization only in the range $2\theta=8$–14°. An example is shown in Figure 3 for the sample iPB**6** with $[rr]=2.8\%$. The sample was first heated to 180 °C and the diffraction profile of the melt was recorded at 180 °C (profile a of Figure 3B). Then, according to the DSC cooling curve of Figure 3A, the sample was rapidly cooled to the crystallization temperature T_{c1}, corresponding to the onset of the crystallization in the DSC scan, and the diffraction profiles were recorded at collecting rate of 1.2 degree min^{-1}, every 5 min in the range $2\theta=8$–14° up to the complete crystallization at T_{c1} (Figure 3C). Similar experiments were performed at crystallization temperatures T_c lower than T_{c1} up to 25 °C (Figure 3D).

The sample iPB**6** crystallizes by cooling the melt to −30 °C completely in form I, as indicated by the diffraction profile b of Figure 3B, which shows the $(110)_I$, $(300)_I$, and $(220)_I+(211)_I$ reflections of form I at $2\theta=9.9$, 17.3, and 20.5°, respectively. The diffraction profiles recorded at 55 °C during the crystallization at 55 °C of Figure 3C clearly show that, starting from the amorphous halo of the melt (crystallization time of 0 min in Figure 3C), the $(110)_I$ reflection of form I at $2\theta=9.9$° appears at the beginning of the crystal-

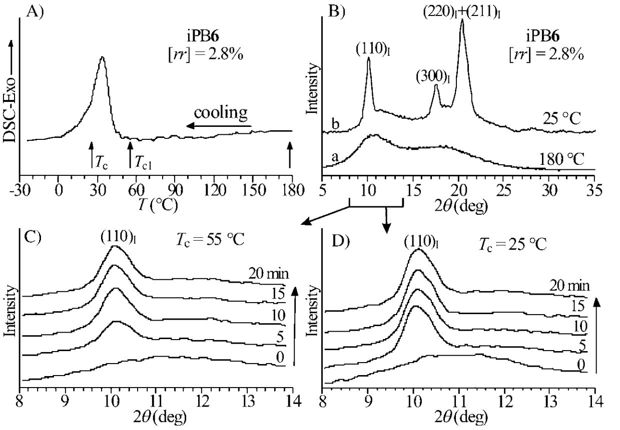

Figure 3. A) DSC (differential scanning calorimetry) cooling curve from the melt at 2.5 °C min^{-1}. Exo = exotherm. B) X-ray powder diffraction profiles recorded at 180 °C (melted sample) and 25 °C of the sample iPB**6** with $[rr] = 2.8$ mol%. The $(110)_{\mathrm{I}}$, $(300)_{\mathrm{I}}$, and $(220)_{\mathrm{I}} + (211)_{\mathrm{I}}$ reflections of form I at $2\theta = 9.9$, 17.3, and 20.5°, respectively, are indicated in (B). In (A) the arrows indicate the temperatures at which the diffraction profiles were recorded (180, 55, and 25 °C). C,D) X-ray powder diffraction profiles recorded in the range $2\theta = 8$–14° at the crystallization temperatures 55 °C (C) and 25 °C (D) during the isothermal melt-crystallization. The crystallization times are also indicated.

lization (5 min), when the $(200)_{\mathrm{II}}$ reflection at $2\theta = 11.9°$ of form II is not observed. The intensity of the reflection of form I increases during the crystallization, and the $(200)_{\mathrm{II}}$ reflection of form II at $2\theta = 11.9°$ never appears.

At 25 °C, the crystallization is faster and only the $(110)_{\mathrm{I}}$ reflection of form I appears and no crystals of form II form during crystallization. These data clearly indicate that for the stereoirregular sample iPB**6** crystals of form I are obtained directly from melt crystallization and not from a rapid transformation by aging at room temperature of the crystals of form II formed from the melt crystallization. Similar experiments were performed for all samples of Figure 2 (see the Supporting Information) and confirmed that less stereoregular iPB samples with *rr* content higher than 2 % crystallize from the melt directly into form I.

The presence of *rr* stereodefects favors the crystallization from the melt of the stable form I over that of form II, which is the kinetically favored modification in highly isotactic samples. This may be due to the reduced stability of the 11_3 helical conformation of form II in the presence of high concentrations of *rr* defects, relative to the 3_1 helical conformation of form I, or the increased crystallization rate of form I because of the increased flexibility of the chains in the presence of *rr* defects.

The discovery that incorporation of *rr* stereodefects produces direct crystallization of the stable form I of iPB may be the key for a broader future development of iPB. The problem of occurrence of form II to form I transformation is solved. Furthermore, incorporation of *rr* defects produces only a slight decrease of crystallinity, from values of 60–70 % of the most isotactic samples to remarkable values of 40–50 % of the more stereodefective samples that crystallize form the melt in form I (Table 1). This result guarantees that the outstanding mechanical properties of strength and flexibility of iPB are maintained even in stereodefective samples. The stress–strain curves of some iPB samples are reported in Figure 4, as an example. The curves of melt-crystallized samples are compared with those of samples aged at room temperature for at least 1 month to allow complete transformation of form II into form I for the most isotactic samples.

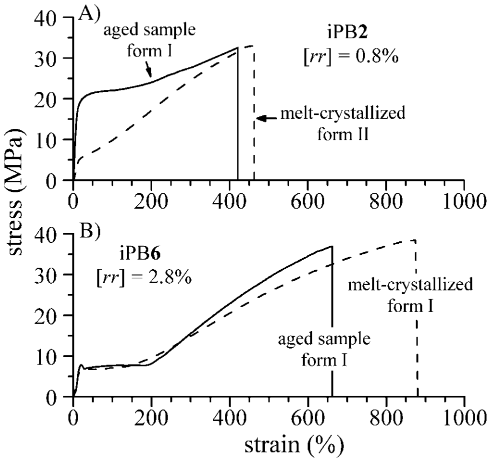

Figure 4. Stress–strain curves of melt-crystallized compression molded films of samples iPB**2** with $[rr] = 0.8$ % (A) and iPB**6** with $[rr] = 2.8$ % (B) before (dashed lines) and after (continuous lines) aging at room temperature for 1 month.

It is apparent that the increase of concentration of *rr* defects does not produce a strong decrease of strength and modulus (the Young modulus of melt-crystallized samples varies from 60–70 MPa of the most isotactic samples iPB**1**–**4** that are crystallized in form II, to 40–60 MPa of the irregular samples iPB**5**–**8** that are crystallized in form I), but produces an increase of deformation at break and, hence, an improvement of flexibility and ductility. Moreover, most importantly, while in the most isotactic samples (as in Ziegler–Natta iPBs) aging at room temperature produces a change of the mechanical properties owing to the transformation of form II into form I (Figure 2 B) (a net increase of modulus and stress at yielding is observed in the stress–strain curves of Figure 4 A), in stereodefective samples no alteration of the mechanical properties is observed upon aging (Figure 4 B) because of the absence of the phase transformation.

In conclusion, single-center metalloorganic catalysis has allowed the synthesis of iPB samples of controlled molecular structure that are used as model systems for understanding the influence of *rr* stereodefects on the thermodynamic stability and crystallization kinetics of polymorphic forms of iPB. Moreover, the discovery that incorporation of *rr* stereodefects produces direct crystallization of the stable form I of iPB might also have a practical interest. In fact, in contrast to highly isotactic samples, melt-crystallized specimens of stereodefective iPB samples do not undergo phase transformation upon aging at room temperature, so that the undesirable effects, such as shrinkage of the molded objects generated by densification, generally observed in Ziegler–Natta iPBs, are eliminated.

It is worth pointing out that the current manufacturing process of polybutene is a continuous solution polymerization process in neat liquid 1-butene: this process implies that, as the polymer is fully dissolved in the liquid monomer, particle polymer morphology is not an issue, and hence catalysts do not need to be heterogenized. We recall that the latter aspect has been the main hindrance in the development of metallocene catalysts for polypropylene, which is manufactured in either slurry or gas-phase processes, in which control over particle morphology is a fundamental aspect of catalyst design, in order to avoid reactor fouling and fines formation. This process has the unique ability to produce polymer particles of controlled spherical morphology directly in the reactor, thanks to a full replication of the spherical catalyst particles.[10] In the case of butene polymerization, on one hand the solution process does not require catalyst heterogenization and no limitations in catalyst performance have been found, and on the other hand a solution to the problems related to the form II to form I transition that have prevented the commercial diffusion of iPB has been found. The possible success of metallocene catalysts in the industrial production of polybutenes is therefore not a question of catalyst performance, but rather one of applications and market development.

Received: August 1, 2009
Revised: October 18, 2009

Keywords: crystallization · isotactic polybutenes · metallocenes · polymerization

---

[1] H. H. Brintzinger, D. Fischer, R. Mulhaupt, B. Rieger, R. M. Waymouth, *Angew. Chem.* **1995**, *107*, 1255; *Angew. Chem. Int. Ed. Engl.* **1995**, *34*, 1143.
[2] L. Resconi, L. Cavallo, A. Fait, F. Piemontesi, *Chem. Rev.* **2000**, *100*, 1253.
[3] a) C. De Rosa, F. Auriemma, A. Di Capua, L. Resconi, S. Guidotti, I. Camurati, I. E. Nifant'ev, I. P. Laishevtsev, *J. Am. Chem. Soc.* **2004**, *126*, 17040; b) C. De Rosa, F. Auriemma, *J. Am. Chem. Soc.* **2006**, *128*, 11024; c) C. De Rosa, F. Auriemma, O. Ruiz de Ballesteros, L. Resconi, I. Camurati, *Chem. Mater.* **2007**, *19*, 5122.
[4] L. Resconi, S. Guidotti, I. Camurati, R. Frabetti, F. Focante, I. E. Nifant'ev, I. P. Laishevtsev, *Macromol. Chem. Phys.* **2005**, *206*, 1405.
[5] G. Natta, P. Corradini, I. W. Bassi, *Nuovo Cimento Suppl.* **1960**, *15*, 52.
[6] A. Turner-Jones, *J. Polym. Sci. Part B* **1963**, *1*, 455.
[7] V. Petraccone, B. Pirozzi, A. Frasci, P. Corradini, *Eur. Polym. J.* **1976**, *12*, 323.
[8] L. Luciani, J. Seppälä, B. Löfgren, *Prog. Polym. Sci.* **1988**, *13*, 37.
[9] L. Resconi, I. Camurati, F. Malizia, *Macromol. Chem. Phys.* **2006**, *207*, 2257.
[10] E. P. Moore, *Polypropylene Handbook*, Hauser, Munich, **1996**.